Surg Endosc (2014) 28:933–940
DOI 10.1007/s00464-013-3249-0

Real-time image guidance in laparoscopic liver surgery: first clinical experience with a guidance system based on intraoperative CT imaging

Hannes G. Kenngott · Martin Wagner · Matthias Gondan · Felix Nickel · Marco Nolden · Andreas Fetzer · Jürgen Weitz · Lars Fischer · Stefanie Speidel · Hans-Peter Meinzer · Dittmar Böckler · Markus W. Büchler · Beat P. Müller-Stich

Received: 2 April 2013 / Accepted: 4 October 2013 / Published online: 1 November 2013

Abstract
Background Laparoscopic liver surgery is particularly challenging owing to restricted access, risk of bleeding, and lack of haptic feedback. Navigation systems have the potential to improve information on the exact position of intrahepatic tumors, and thus facilitate oncological resection. This study aims to evaluate the feasibility of a commercially available augmented reality (AR) guidance system employing intraoperative robotic C-arm cone-beam computed tomography (CBCT) for laparoscopic liver surgery.
Methods A human liver-like phantom with 16 target fiducials was used to evaluate the Syngo iPilot® AR system. Subsequently, the system was used for the laparoscopic resection of a hepatocellular carcinoma in segment 7 of a 50-year-old male patient.
Results In the phantom experiment, the AR system showed a mean target registration error of 0.96 ± 0.52 mm, with a maximum error of 2.49 mm. The patient successfully underwent the operation and showed no postoperative complications.
Conclusion The use of intraoperative CBCT and AR for laparoscopic liver resection is feasible and could be considered an option for future liver surgery in complex cases.

Keywords Navigation · Liver surgery · Liver resection · Augmented reality · Intraoperative imaging · Computer assistance

H. G. Kenngott (✉) · M. Wagner · F. Nickel · J. Weitz · L. Fischer · M. W. Büchler · B. P. Müller-Stich
Department of Surgery, University of Heidelberg, Im Neuenheimer Feld 110, 69120 Heidelberg, Germany
e-mail: hannes.kenngott@med.uni-heidelberg.de

B. P. Müller-Stich
e-mail: Beat.Mueller@med.uni-heidelberg.de

M. Gondan
Institute of Medical Biometry and Informatics, University of Heidelberg, Im Neuenheimer Feld 305, 69120 Heidelberg, Germany

M. Nolden · A. Fetzer · H.-P. Meinzer
Division of Medical and Biological Informatics, German Cancer Research Centre, Im Neuenheimer Feld 280, 69120 Heidelberg, Germany

S. Speidel
Institute for Anthropomatics IFA, Karlsruhe Institute of Technology KIT, Adenauerring 2, 76131 Karlsruhe, Germany

D. Böckler
Department of Vascular and Endovascular Surgery, University of Heidelberg, Im Neuenheimer Feld 110, 69120 Heidelberg, Germany

Liver malignancies are one of the main causes of death in cancer-afflicted patients. Primary liver cancer, such as hepatocellular carcinoma (HCC) and cholangiocellular carcinoma, contributes to this, as do liver metastases, mainly from colorectal carcinoma [1]. Of the available options (chemotherapy, radiotherapy, ablative therapy), surgery is considered to be the key treatment for a curative approach.

However, the liver is an organ with a complex and highly distinct anatomy. Performing liver resection is therefore a challenge, requiring expertise and years of training. Computer-assisted surgery may be able to reduce this complexity. Today, computer-based systems for liver surgery focus on three main issues: preoperative planning, intraoperative navigation, and postoperative control. Preoperative planning allows for three-dimensional (3D) visualisation of internal structures based on radiological imaging. Intraoperative navigation involves the transfer of

the preoperative planning into the operating room and visualizes the computer model in relation to both the patient's liver and the surgical instruments. Postoperative control is used for the treatment evaluation and follow-up procedure. Peterhans et al. [2] and Najmaei et al. [3] both provide a good overview of this domain.

To use intraoperative navigation, six main steps are necessary: a preoperative image (computed tomography [CT], magnetic resonance imaging [MRI]) has to be segmented to identify important structures, such as vessels and the tumor [4]. After preoperative planning, the operation can be performed and the 3D planning data needs to be registered to the patient anatomy [5]. By tracking the surgical instruments, a digital and 3D representation of the surgical field, with the internal anatomy of the liver and the surgical instruments, can be established and visualized.

The main drawback of this approach for liver surgery is the movement and deformation of the soft tissue due to surgical access (laparotomy or laparoscopy with pneumoperitoneum), breathing, heartbeat, iatrogenic manipulation, and tissue dissection, all of which alter the position and anatomy of the liver [6, 7].

To account for this problem, it is either possible to measure all forces that deform the liver and predict the behavior of the tissue based on a biomechanical model of tissue deformation, or to use intraoperative imaging to continuously update the image. In this paper, we propose the use of robotic C-arm cone-beam CT (CBCT) in a hybrid operating room for computer-assisted guidance during laparoscopic resection for liver cancer.

Materials and methods

The experiments were performed using an Artis Zeego™ multi-axis system in a hybrid operating room setting (Siemens Healthcare Sector, Forchheim, Germany), which is normally used for endovascular surgery and transapical valve replacement. We used the built-in augmented reality (AR) guidance system Syngo iPilot® (Siemens Healthcare Sector, Forchheim, Germany). After the acquisition of intraoperative CBCT, this software enabled volume registration to generate a real-time overlay of CBCT data on the fluoroscopy, in addition to highlighting important structures and features, such as vessels or resection planes, in order to guide the surgeon.

Accuracy of AR guidance

Before the clinical evaluation took place, phantom experiments were carried out to test the reliability of the system. To analyse the error in the AR guidance system, two different experiments were performed using a modular, customized, human-like phantom based on real human CT data. For the experiment, the body cavity and the liver of the phantom were used. Sixteen glass beads were inserted into the liver as target fiducials directly under the surface (Fig. 1).

First, the registration error of the guidance system itself was evaluated. After acquiring a CBCT and subsequent volume visualization, the AR guidance was tested from different angles: in the craniocaudal axis from −40° to 40° in 10° steps, and in the left–right axis from −90° to 90° in steps of 15°, respectively. These angles were chosen as feasible values to allow for the detailed assessment of possible positions. In total, it was possible to assess 117 angle combinations. By comparing the volume visualization and the fluoroscopy position, the target registration error (TRE; defined as the distance between the real position of the targets and their virtual AR visualization) of the 16 targets for each angle could be measured using the DICOM viewer MicroDicom (Simeon Stoykov, Sofia, Bulgaria; [8]). The findings were analyzed with descriptive statistics (mean, standard deviation [SD], and maximum error) using the statistical computing environment R [9].

Accuracy of the surgeon

Second, surgical error was evaluated as a parameter to measure the accuracy and precision that the surgeon could achieve when a target was hit under fluoroscopic guidance. Therefore, the surgeon aimed for eight of the targets, five times each, with the only guidance being the fluoroscopy. The distance to the target was then measured. This was performed from both an optimal angle vertical to the surface of the liver and as an angle considered to be the worst case in liver surgery that differed 30° in both the craniocaudal and the left–right axes. This was done to evaluate the extremes of possible positions. The findings were analysed with descriptive statistics (mean, SD, and maximum error) using the statistical computing environment R [9].

Clinical integration of the system

After the phantom experiments were completed with good accuracy, these results were then implemented into the procedure for a 50-year-old male patient with histologically proven HCC of segment 7 who underwent laparoscopic operation with an atypical segmental resection. The need for ethics committee approval was carefully considered. However, upon consultation, the local ethics committee deemed a votum, in this particular case of a proof of principle, not necessary. Following good clinical practice, the patient was thoroughly informed regarding all details of the planned procedure, in particular concerning the aspect

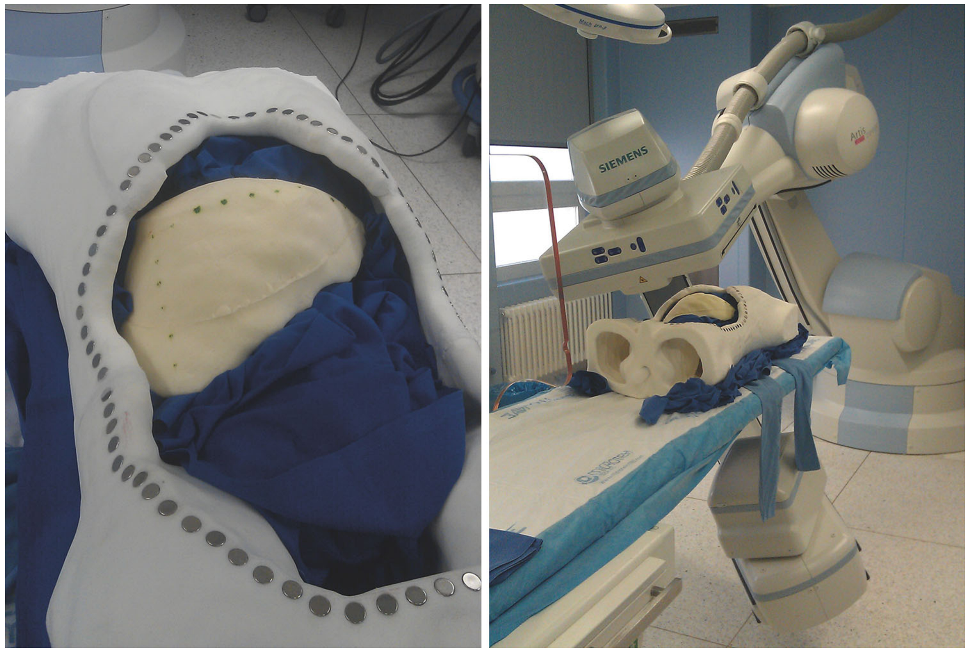

Fig. 1 *Left* laparoscopic phantom with liver and targets. The position of the embedded glass targets is marked on the surface. *Right* phantom with robotic C-arm in the hybrid operating room

of radiation exposure. Written informed consent was then obtained. For safety reasons, a patient was selected whose tumor was located close to the liver surface. The tumor was therefore readily accessible and the operation could therefore be performed without computer assistance. The laparoscopic liver resection was performed in a standardized way, with the only difference being immobilization of the patient using a vacuum mattress and intraoperative imaging with CBCT and fluoroscopic guidance.

The operation was undertaken in a hybrid operating room that is typically used for endovascular surgery and transapical valve interventions. The hybrid operating room contained an industrial robot that allowed for easy and reproducible positioning of the mounted CBCT via remote control (Artis Zeego^{TM}, Siemens Healthcare Sector, Forchheim, Germany). The corresponding radiological workstation, Syngo X Workplace^{TM} (Siemens Healthcare Sector, Forchheim, Germany), which was implemented in the operating room, was used to process the acquired images.

Access to the abdominal cavity was obtained by means of four ports: (i) Paraumbilical, (ii) 5 cm left of the umbilicus, (iii) the subxiphoid region, and (iv) right of the umbilicus in the right anterior axillary line, with ports 1 and 2 having a diameter of 12 mm, and ports 3 and 4 a diameter of 5 mm (see Gumbs et al. [10]). After the liver was mobilized, the tumor was exposed and the ligamentum falciforme was sewn to the abdominal wall, thereby stabilizing the liver in a position that rendered the tumor accessible without manipulation following the intraoperative imaging. An endoscopic clip on the liver surface allowed for a gating technique to account for respiratory movement in the later course; the surgeon only used the fluoroscopic information when this marker was found in the same state that it had previously been in the breathing cycle.

For intraoperative imaging, the C-arm was moved from its resting position to the surgical table. With a foot control switch, the surgeon used fluoroscopic guidance to position the C-arm above the liver. For the CBCT, a protocol of 8 s was used in which the C-arm rotated around the patient and acquired a series of images that were translated into tomographic scans (Fig. 3). At the workstation, the CT image was opened and settings for volume visualization were selected. As the HCC was poorly visible in CT imaging, a preoperative MRI was registered to the intraoperative CT. The preoperative MRI was therefore loaded from the Picture Archiving and Communication System and registered semi-automatically to the CBCT. This allowed for visualization of the tumor in its intraoperative position, even when it was not visible on the CBCT.

The resulting 3D model of liver, tumor, and gating clip were used for AR guidance. After determining the appropriate resection margin on the liver surface under gated fluoroscopic guidance, the resection was performed with the Ultracision^{TM} harmonic scalpel (Ethicon GmbH, Hamburg, Germany).

Results

Accuracy of AR guidance

It was possible to test the AR system from 97 of the 117 different angles (82.9 %). A total of 20 angles could not be

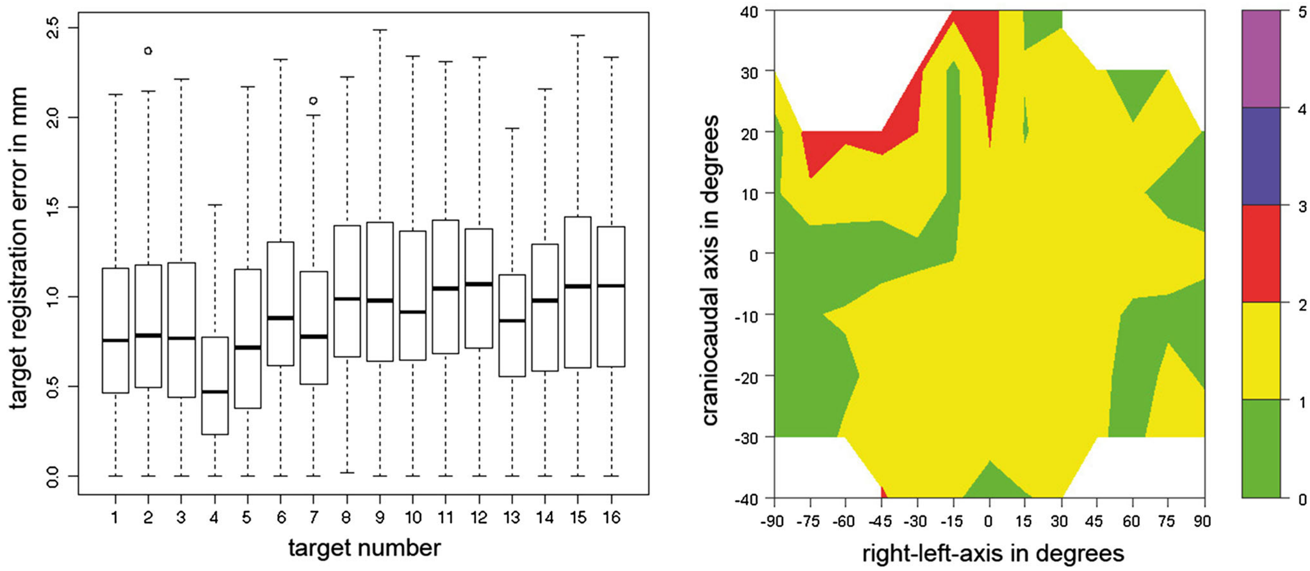

Fig. 2 Results of the phantom experiments. *Left* error depending on target position on the liver surface: results for all 16 targets. *Right* maximal error depending on angle of fluoroscopy: distribution over all angles of robot position. Blank fields were not possible to obtain

assessed due to the robot or CBCT colliding with either the surgical table or the patient phantom (empty areas in Fig. 2). Of the resulting 1,552 targets, 1,427 were evaluated (91.9 %), since the remaining targets were covered by other targets or radiopaque structures of the phantom, thereby preventing a precise measurement of distances.

The overall mean TRE was 0.93 mm (SD 0.54 mm), with a maximum of 2.49 mm. The mean error ranged from 0.53 mm (SD 0.39 mm, target 4) to 1.1 mm (SD 0.55 mm, target 12) when each of the 16 targets was analyzed separately over all angles. Analysis of the error, independent of the angles in both axes, revealed a homogenous distribution of the maximal error for the different angles. A summary of the results can be seen in Fig. 2.

Accuracy of the surgeon

The experiment testing the accuracy of the surgeon resulted in a mean distance to target of 0.45 mm (SD 0.60 mm) for the optimal angle and 1.25 mm (SD 1.01 mm) for the most abysmal angle, respectively. Furthermore, a ratio of 60 % perfect hits (error = 0 mm) was found at the optimal angle, compared with 17.5 % for the most abysmal angle. The surgeon described the targeting as being much more difficult when performed from the most abysmal angle.

Clinical integration of the system

The clinical integration of the system was successful (Fig. 3). During the operation there were no signs of peritoneal carcinosis or spread of cancer. The operative time was 135 min, with a blood loss of 300 ml. During the laparoscopic preparation of the tumor, the surgeon used fluoroscopy to navigate the instruments to the predefined resection margin (Fig. 4).

Fig. 3 Acquiring intraoperative image data with the robotic cone beam computed tomography

Fluoroscopy and CBCT images could be overlaid with the 3D model of the liver, which allowed for precise virtual preparation and visualization of the tumor, including the appropriate safety margin. The fluoroscopy, along with the preoperative resection plan and the laparoscopic video, could be displayed on a flat-screen panel in an ergonomic position for the surgeon (Fig. 5).

A specimen of 5.5 × 3.3 × 2.2 cm containing the tumor (1.6 cm in diameter) was removed, and the pathological report confirmed both an HCC (pT1, pNx, G2) based on a chronic hepatitis C and a tumor-free resection margin (R0). There were no intra- or postoperative complications related to the operation. Up until 9 months postoperatively, the

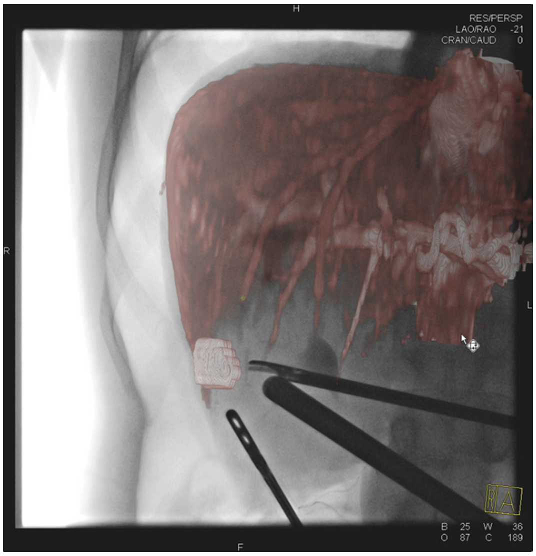

Fig. 4 Fluoroscopy with augmented reality: the preoperative magnet resonance imaging data were superimposed on the real-time fluoroscopy, with the surgical instruments clearly visible in relation to the tumor

Fig. 5 Setup in the hybrid operation room during the actual laparoscopic intervention, with visualization of fluoroscopy, fluoroscopy overlay, imaging data, planning data, data of the patient, and laparoscopic view

patient showed no sign of recurrent tumor in MRI scans or elevated tumor markers.

Discussion

To our knowledge, this paper describes the first attempt to use intraoperative CBCT for navigated laparoscopic liver surgery in a real operation. It covers two different aspects. First, we evaluated a commercially available AR system and its use for guidance in laparoscopic liver surgery. Second, we introduced intraoperative CT imaging into general surgery via CBCT.

The overall error of the Syngo iPilot® AR system is threefold: (i) the internal registration error of the robotic fluoroscopy system, (ii) the cyclic movement of the liver due to respiration and (iii) the targeting error of the surgeon when marking the resection line under fluoroscopic guidance.

Error (i) was fairly low in the phantom experiments, with a maximum error of 2.5 mm considering all possible angles and all parts of the liver surface. This maximum error was generally constant over all possible angles. Nevertheless, the extremely cranial angles on the right showed slightly higher errors, as did some impossible angles. However, this position of the robotic arm might be the most ergonomic for a surgeon operating from the left side of the patient. Error (ii) was not assessed in this study, though liver motion owing to respiration was noted to be low after pneumoperitoneum was established. To evaluate this error thoroughly, we performed animal studies, which are to be published in a different study. The experiment evaluating surgical targeting accuracy (iii) revealed that the angle to the liver surface was critical and contingent on the surgeon's aiming performance. In addition to the objectively measured increase in the targeting error, the surgeon in the phantom experiment subjectively described the aiming period as being much more difficult and prolonged when working on a bad angle. Combining both findings, the angle of the fluoroscopy should be chosen in optimal relation to the liver surface, as this has a much greater influence on accuracy than does the internal registration error of the guidance system.

To compare the value of navigated laparoscopic surgery with existing solutions, the proposed AR system and the intraoperative CBCT have to be considered in terms of human–machine interface, validity of imaging, and clinical feasibility.

Human–machine interface

Apart from representation as (transversal) slices, 3D volume visualization is the simplest way to present tomographic images to the surgeon. Nozaki et al. [11, 12] proved the feasibility of volume visualization of CBCT for laparoscopic urological and retroperitoneal surgery. However, they leave it to the surgeon to transfer the imaging information to the surgical field. The AR system that we have described, on the other hand, allows for visualization of the surgical instruments in relation to the anatomy. This information could, therefore, further increase the confidence of the surgeon, which is already boosted by the CBCT, described by Nozaki et al. This has already been found to be useful in neurovascular interventions, especially in complex cases of cerebral aneurysms [13].

Nonetheless, in laparoscopic surgery, surgeons must divide their attention to retrieve information from the two visualizations, laparoscopic image, and AR fluoroscopy. The next step towards improving the human–machine interface would be an AR directly in the laparoscopic video, which has been demonstrated with conventional preoperative CT without fluoroscopy for pediatric splenectomy [14], liver surgery [15, 16], and urology [17, 18]. Although these AR systems are able to provide a sound and reliable human–machine interface, they have drawbacks, such as limited reliability and usability, which is discussed below.

Validity of imaging and clinical feasibility

The main drawback of image guidance in laparoscopic surgery is the limited validity of the preoperative imaging due to the intraoperative deformation and movement of organs. Although the navigation system for laparoscopic splenectomy in pediatric surgery by Ieiri et al. [14] delivered sufficient results for visualization of the splenic vascular anatomy, it was not adapted to organ deformation and nor does it deliver real-time information in terms of intraoperative images. Nicolau et al. [15] described a method for camera-based AR in liver surgery, with a manual image registration by the user, but clearly stated that the feasibility remained strictly limited to small fields of interest, due to the rigid and clinically unfeasible registration of preoperative images. The deformable and interactive AR proposed by Vemuri et al. [17] allowed for compensation of organ shift and deformation (error (ii), see above), but required manual deformation updates and thus is very time consuming and impractical for an operating room setting. All authors agree on the need for automatic and real-time soft tissue deformation compensation. As described in detail in Nicolau et al. [15], there are two main strategies to account for organ motion: one is the non-rigid registration of preoperatively acquired images to organ surfaces reconstructed from endoscopic information (such as time of flight, stereo-endoscopy, structure from motion, and so on). The second is intraoperative imaging. Due to low cost and absence of radiation exposure, most of the work focuses on laparoscopic ultrasound, and the surgical community also anticipates its use in navigated surgery [19]. Nevertheless, the disadvantages of ultrasound, such as poor image quality, dependence on the user's expertise and the restriction of field of view, remain unsolved. Furthermore, in this approach, image acquisition has to be repeated following organ deformation.

Shekhar et al. [16]. address all these problems with a CT-based live AR. They conducted laparoscopic liver surgery on pigs within a conventional CT scanner. Continuous low-dose CT images allowed for registration of the preoperative diagnostic CT scan, which would then provide the desired live information on organ deformation; unfortunately, these image sequences were far from being real time due to technical limitations. In contrast with the CBCT in the present publication, the authors relied, for their animal trial, on a conventional CT scanner, which might provide better quality at lower acquisition time but is usually not present in an operating room. A built-in spiral CT scanner would require much larger operating rooms and is in contrast with CBCT due to its technical design limiting mobility at the operation table.

Teber et al. [18] used intraoperative CT imaging with a mobile C-arm. This allowed them to provide very accurate image guidance. However, their approach to AR was different: they used inside-out tracking by inserting special markers on the organ surface before CT imaging that could be optically retrieved from the laparoscopic image. In addition, Rassweiler et al. [20] found no significant limitation in image quality by the introduction of surgical instruments. This promising approach would benefit from the robotic CBCT due to easier handling than a mobile C-arm and better imaging quality and volume visualization.

An important drawback of our suggested method is the use of CBCT, which causes additional radiation exposure for the patient. However, additional radiation exposure was judged to be marginal in the present case. As shown by [21], a CBCT has a radiation exposure of about 7 mSv for an 8 s scan and showed significantly less radiation than a standard CT scan of the abdominal cavity, which resulted in a radiation dose of about 8 mSv. In addition, in this study we used a novel CBCT protocol by Siemens, which resulted in even lower radiation exposure. During its maturation as a product, CBCT has gradually shown less radiation exposure at better or similar imaging quality. This process is likely to continue. The procedure and the need for an additional CBCT resulting in additional radiation exposure at the level of a conventional abdominal CT scan and the potential risk of the use of iodine contrast agent was thoroughly discussed with the patient, who gave his informed consent.

Other possibilities would be to use other registration techniques to register the pre-procedural image data. Land marker-based registration is one possible solution requiring a tracking system in the operating room. Magnetic and optic tracking were both used by our group to evaluate feasibility in the operating room. Both systems have certain drawbacks. While optical systems require direct line of sight, magnetic systems are very susceptible to contortion and error due to ferromagnetic metals in the magnetic field [22, 23]. One of the most important problems is that the pre-procedural CT is not adapted when tissue is dissected or moved. CBCT, on the other hand, can be performed again when needed to acquire intraoperative data. However, the need to leave the operating room while performing a CBCT limits this technique.

Intraoperative ultrasound is another alternative to register preoperative data and is widely adopted [19]. Although deep-lying metastases or air in between the target and risk structures leads to missing data. In addition, the reliability and accuracy of intraoperative ultrasound is highly dependent on the experience of the user. Intraoperative MRI might be a solution that does not result in radiation exposure and does not need iodine contrast agents. However, intraoperative MR tomographs require non-ferromagnetic instruments and equipment as well as caution before entering the room. The ideal combination of imaging and registration has yet to be found.

To conclude, we have shown the feasibility of using CBCT in the surgical workflow. AR fluoroscopy provides an intuitive human–machine interface for accurate image guidance. Given the promising examples from literature, future options and applications for the use of intraoperative CBCT arise. One of the main advantages of the hybrid operating room is the integrated environment. The CBCT and the surgical setup such as the operating table were intrinsically calibrated. Novel protocols could also lead to sufficient real-time imaging in cases where CBCT still lacks imaging quality [24]. Moreover, innovative approaches for continuous motion compensation, such as inside-out tracking or trajectory estimation of the breathing cycle [25], could be implemented into the system. The goal will be to improve the surgeon's orientation regarding target and risk structures for more complex laparoscopic operations such as more central tumors in the liver.

Acknowledgments The authors thank Siemens AG, Healthcare Sector, for providing expert personnel during the evaluation to calibrate and operate the system during the intervention. In particular, we would like to thank Martin von Roden for his excellent contribution. Professor Böckler received a research grant and speaker honoraria from Siemens AG. Dr. Müller-Stich received reimbursements of travel expenses from Siemens AG, Erlangen, Germany. This research was supported by the Transregional Collaborative Research Centre (TCRC) 'Cognition-Guided Surgery' and the Research Training Group 1126 both funded by the DFG (German Research Foundation).

Disclosures Drs. Kenngott, Wagner, Gondan, Nickel, Nolden, Fetzer, Weitz, Fischer, Meinzer and Büchler have no conflicts of interest or financial ties to disclose.

References

1. Jemal A, Bray F, Center MM, Ferlay J, Ward E, Forman D (2011) Global cancer statistics. CA Cancer J Clin 61(2):69–90
2. Peterhans M, Oliveira T, Banz V, Candinas D, Weber S (2012) Computer-assisted liver surgery: clinical applications and technological trends. Crit Rev Biomed Eng 40(3):199–220
3. Najmaei N, Mostafavi K, Shahbazi S, Azizian M (2012) Image-guided techniques in renal and hepatic interventions. Int J Med Robot. doi:10.1002/rcs.1443
4. Oliveira DA, Feitosa RQ, Correia MM (2011) sation of liver, its vessels and lesions from CT images for surgical planning. Biomed Eng Online 10:30
5. Nam WH, Kang DG, Lee D, Lee JY, Ra JB (2012) Automatic registration between 3D intra-operative ultrasound and pre-operative CT images of the liver based on robust edge matching. Phys Med Biol 57(1):69–91
6. Zijlmans M, Langø T, Hofstad EF, Van Swol CFP, Rethy A (2012) Navigated laparoscopy—liver shift and deformation due to pneumoperitoneum in an animal model. Minim Invasive Ther Allied Technol 21(3):241–248
7. Bussels B, Goethals L, Feron M, Bielen D, Dymarkowski S, Suetens P, Haustermans K (2003) Respiration-induced movement of the upper abdominal organs: a pitfall for the three-dimensional conformal radiation treatment of pancreatic cancer. Radiother Oncol 68(1):69–74
8. Stoykov SA. Micro Dicom viewer. http://www.microdicom.com. Accessed June 2013
9. R Core Team (2012) R: a language and environment for statistical computing. R Foundation for Statistical Computing, Vienna. http://www.R-project.org. Accessed June 2013
10. Gumbs AA, Gayet B, Gagner M (2008) Laparoscopic liver resection: when to use the laparoscopic stapler device. HPB (Oxf) 10(4):296–303
11. Nozaki T, Iida Y, Morii A, Fujiuchi Y, Fuse H (2012) Laparoscopic radical nephrectomy under near real-time three-dimensional surgical navigation with C-arm cone beam computed tomography. Surg Innov 19(3):263–267
12. Nozaki T, Fujiuchi Y, Komiya A, Fuse H (2013) Efficacy of DynaCT for surgical navigation during complex laparoscopic surgery: an initial experience. Surg Endosc 27(3):903–909
13. Rossitti S, Pfister M (2009) 3D road-mapping in the endovascular treatment of cerebral aneurysms and arteriovenous malformations. Interv Neuroradiol 15(3):283–290
14. Ieiri S, Uemura M, Konishi K, Souzaki R, Nagao Y, Tsutsumi N, Akahoshi T, Ohuchida K, Ohdaira T, Tomikawa M, Zanoue K, Hashizume M, Taguchi T (2012) Augmented reality navigation system for laparoscopic splenectomy in children based on preoperative CT image using optical tracking device. Pediatr Surg Int 28(4):341–346
15. Nicolau S, Soler L, Mutter D, Marescaux J (2011) Augmented reality in laparoscopic surgical oncology. Surg Oncol 20(3):189–201
16. Shekhar R, Dandekar O, Bhat V, Philip M, Lei P, Godinez C, Sutton E, George I, Kavic S, Mezrich R, Park A (2010) Live augmented reality: a new visualization method for laparoscopic surgery using continuous volumetric computed tomography. Surg Endosc 24(8):1976–1985
17. Vemuri AS, Wu JCH, Liu KC, Wu HS (2012) Deformable three-dimensional model architecture for interactive augmented reality in minimally invasive surgery. Surg Endosc 26(12):3655–3662
18. Teber D, Guven S, Simpfendörfer T, Baumhauer M, Güven EO, Yencilek F, Gözen AS, Rassweiler J (2009) Augmented reality: a new tool to improve surgical accuracy during laparoscopic partial nephrectomy? Preliminary in vitro and in vivo results. Eur Urol 56(2):332–338
19. Våpenstad C, Rethy A, Langø T, Selbekk T, Ystgaard B, Hernes TA, Marvik R (2010) Laparoscopic ultrasound: a survey of its current and future use, requirements, and integration with navigation technology. Surg Endosc 24(12):2944–2953
20. Rassweiler MC, Ritter M, Michel MS, Häcker A (2013) Influence of endourological devices on 3D reconstruction image quality using the Uro Dyna-CT. World J Urol 31(5):1291–1295
21. Bai M, Liu B, Mu H, Liu X, Jiang Y (2012) The comparison of radiation dose between C-arm flat-detector CT (DynaCT) and multi-slice CT (MSCT): a phantom study. Eur J Radiol 81(11):3577–3580. http://www.ncbi.nlm.nih.gov/pubmed/21963617
22. Kenngott HG, Wegner I, Neuhaus J, Nickel F, Fischer L, Gehrig T, Meinzer HP, Müller-Stich BP (2013) Magnetic tracking in the

operation room using the da Vinci® telemanipulator is feasible. J Robot Surg 7(1):59–64
23. Kenngott HG, Neuhaus J, Müller-Stich BP, Wolf I, Vetter M, Meinzer HP, Köninger J, Büchler MW, Gutt CN (2008) Development of a navigation system for minimally invasive esophagectomy. Surg Endosc 22(8):1858–1865
24. Koelblinger C, Schima W, Berger-Kulemann V, Wolf F, Plank C, Weber M, Lammer J (2013) C-arm CT during hepatic arteriography tumour-to-liver contrast: intraindividual comparison of three different contrast media application protocols. Eur Radiol 23(4):938–942
25. Worm ES, Høyer M, Fledelius W, Nielsen JE, Larsen LP, Poulsen PR (2012) On-line use of three-dimensional marker trajectory estimation from cone-beam computed tomography projections for precise setup in radiotherapy for targets with respiratory motion. Int J Radiat Oncol Biol Phys 83(1):e145–e151